

## Picosecond Time-resolved Infrared Imaging by a Non-scanning Two-color Infrared Super-resolution Microscope

Makoto Sakai,\*<sup>1</sup> Tsutomu Ohmori,<sup>1</sup> Masataka Kinjo,<sup>2</sup> Nobuhiro Ohta,<sup>2</sup> and Masaaki Fujii\*<sup>1</sup>

<sup>1</sup>Chemical Resources Laboratory, Tokyo Institute of Technology, 4259 Nagatsuta-cho, Midori-ku, Yokohama 226-8503

<sup>2</sup>Research Institute for Electronic Science, Hokkaido University, N12 W6, Kita-ku, Sapporo 060-0812

(Received August 31, 2007; CL-070942; E-mail: makotos@res.titech.ac.jp)

A non-scanning two-color infrared super-resolution microscope combining a laser fluorescence microscope and picosecond time-resolved transient fluorescence detected IR (TFD-IR) spectroscopy has been developed. Picosecond time-resolved infrared super-resolution images were obtained with 2 ps time resolutions and 1.4  $\mu\text{m}$  spatial resolutions, without XY scanning of the sample or the excitation light of infrared and visible. A demonstration measurement on *Arabidopsis thaliana* roots labeled by Rhodamine 6G is presented.

Molecular vibration is called a “finger print” of molecules, because it sensitively reflects the geometry and circumstance of molecules. If we can map a specific IR absorption band with sub-micron spatial resolution, we will be able to visualize the chemical structure in a nonuniform environment, such as a cell. However, we can never achieve this resolution by the conventional IR mapping method, and thus other analytical methods are used, such as Raman microscopy, in order to achieve a subcellular resolution.<sup>1–3</sup> This is because the spatial resolution of a conventional IR mapping method is limited by the diffraction limit, which is almost the same as the wavelength of light.<sup>4</sup> This diffraction limit prevents conventional IR microscopes from achieving a better spatial resolution, because the IR wavelength is very long, ranging from 3 to 25  $\mu\text{m}$  in the mid-infrared region.

The IR microscope, based on transient fluorescence detected IR (TFD-IR) spectroscopy,<sup>5,6</sup> is capable of breaking the diffraction limit. By using this IR microscope, we can detect the vibrational transition as transient fluorescence from only the spatial region, where both IR and visible light beams are overlapped. By converting IR information into visible fluorescence, we can also increase the spatial resolution to the visible diffraction limit, i.e., the IR is super-resolved.<sup>7</sup>

In the present work, IR and visible light beams were used as illumination light and were irradiated onto a sample. The transient fluorescence from the sample was collected from the opposite side by an objective lens. In this layout, the spatial resolution was determined by the objective NA and the visible fluorescence wavelength; IR super-resolution smaller than the diffraction limit of IR light was achieved. Here, *Arabidopsis thaliana* (*A. thaliana*) roots dyed by Rhodamine 6G were used as a sample. We applied this IR super-resolution microscope to *A. thaliana* root cells and also reported the results of time-resolved measurements.

The laser setup for our two-color IR super-resolution microscope has been described previously.<sup>6,7</sup> Figure 1a shows optical layout used for IR imaging detection. Both IR and visible light with a spectral bandwidth of  $\approx 15\text{ cm}^{-1}$  and a pulse width of  $\approx 3\text{ ps}$ , generated by a picosecond laser system, were introduced into a home-made laser fluorescence microscope. IR and visible

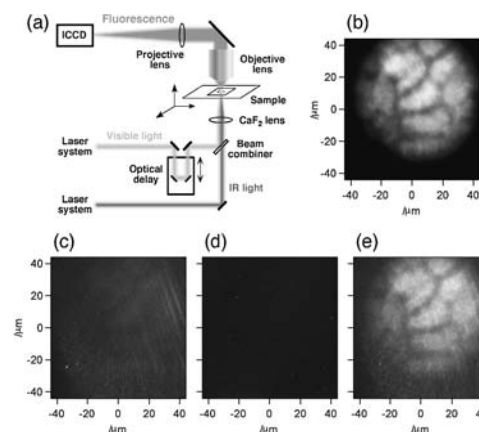


**Figure 1.** (a) Optical layout for IR imaging detection. Picosecond IR and visible light beams are used as the illumination light, and the transient fluorescence is collected from the opposite side by a NA = 0.25 objective lens. (b) Fluorescence image of *A. thaliana* roots labeled by Rhodamine 6G, observed by introducing 539 nm light. (c)–(e) TFD-IR images of *A. thaliana* roots by introducing (c) only visible (wavelength, 607 nm), (d) only IR (wavelength, 3300 nm), and (e) both IR and visible light. Here, a faint image of (c) is a scattering due to the visible light that penetrated a notch filter. The spatial resolution observed from the cross section of the image in figure (e) is almost the same as the diffraction limit of 1.4  $\mu\text{m}$ .

light beams were superposed on a colinear path by a beam-combiner and focused into the sample by a  $\text{CaF}_2$  lens ( $f = 100\text{ mm}$ ). The focal spot sizes of IR and visible light beams were adjusted to about 100  $\mu\text{m}$  at the sample position. Here, *A. thaliana* roots labeled by Rhodamine 6G were used as the sample. During the experiment, IR light with  $< 7\text{ }\mu\text{J/pulse}$  and visible light with  $< 1\text{ }\mu\text{J/pulse}$  irradiated the sample at a repetition rate of 10 Hz. The transient fluorescence from *A. thaliana* roots was collected from the opposite side by a NA = 0.25 objective lens (Newport, M-10X) and was projected onto a CCD camera with an image-intensifier (Princeton Instruments Inc., PI-MAX-1K-HB) and recorded by a personal computer as a fluorescence image. For measuring the time-resolved transient fluorescence detected IR image, the delay time between the IR and visible light beams was varied by an optical delay system (Sigma, LTS-400X). In this layout, picosecond IR and visible light beams were used as the illumination light of a microscope, and the spatial resolution at  $\approx 570\text{ nm}$ , which is a fluorescence wavelength of Rhodamine 6G, was 1.4  $\mu\text{m}$  from the Rayleigh diffraction limit. This is much smaller than the diffraction limit (8.1  $\mu\text{m}$ ) of IR light.

*A. thaliana* seedlings were grown using a  $1 \times 10^{-4}\text{ M}$  ( $\text{M} = \text{mol dm}^{-3}$ ) aqueous Rhodamine 6G solution on a filter

paper of glass fiber. For a preparation of a microscopic specimen, *A. thaliana* roots were crushed between two glass slides after soaking in 1 M HCl in a hot-water bath for 10 min and washed with 45% acetic acid and 3:1 methanol/acetic acid. The preparation was sealed in nujol mull with a cover glass. Rhodamine 6G was purchased from Exciton (R590) and used without further purification.

Figure 1b shows a fluorescence image of *A. thaliana* roots labeled by Rhodamine 6G, observed by introducing 539 nm light. This corresponds to a fluorescence image taken by a conventional fluorescent microscope. As can be seen from the figure, it is clear that Rhodamine 6G dyes the inside of the cell uniformly. Figures 1c–1e show transient fluorescence detected IR (TFD-IR) images of *A. thaliana* roots labeled by Rhodamine 6G, observed by introducing (c) only visible (wavelength, 607 nm), (d) only IR (wavelength, 3300 nm), and (e) both IR and visible light. No fluorescence appears in (c) only visible and (d) only IR. On the other hand, transient fluorescence clearly appears by introducing (e) both IR and visible light, and a TFD-IR image that is almost the same as (b) is observed with a spatial resolution higher than the diffraction limit of IR light. TFD-IR images disappear when the visible light is introduced earlier than the IR light.

We also measured picosecond time-resolved TFD-IR images from  $-10$  to  $50$  ps. Figure 2a shows a demonstration of picosecond time-resolved TFD-IR images around a  $0$  ps delay time. As for these TFD-IR images, a population decay of the vibrationally excited Rhodamine 6G molecule in a cell is demonstrated as the delay-time dependent fluorescence. At a  $-5$  ps delay time when visible light irradiates before IR light, the TFD-IR image is not observed at all. However, at  $0$  ps when visible and IR light irradiates at the same time, a TFD-IR image clearly appears and furthermore decays with time.

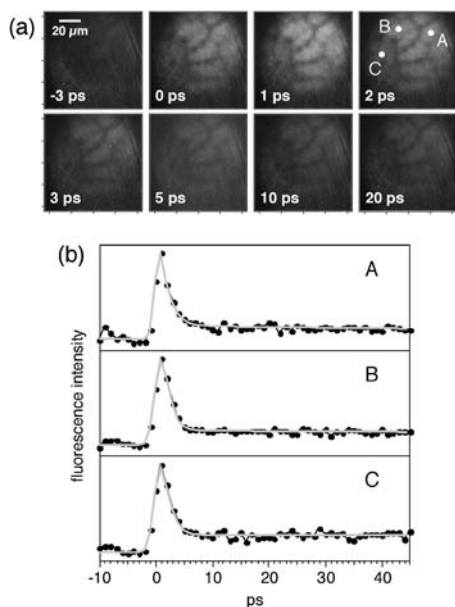


**Figure 2.** (a) Picosecond time-resolved TFD-IR images around a  $0$  ps delay times. (b) Time-profiles of the TFD-IR signal intensity at the point of A–C on the TFD-IR image of (a). The solid line is the best fit to a single-exponential decay convoluted with the instrument response function, and all the decay constant of A–C was estimated to be  $1.5$  ps.

Figure 2b shows time-profiles of the TFD-IR signal intensity at the point of A–C on the TFD-IR image of 2a.

As can be seen in the figure, all of the time-profiles show the same behavior. An interesting feature is that the vibrational energy of Rhodamine 6G is not completely lost, even at a  $50$  ps delay time, which is sufficiently longer than the fast vibrational energy flow with an exponential decay constant of  $1.5$  ps. Many previous reports<sup>5–10</sup> on vibrational relaxation dynamics of similar vibrational energy in a similar molecular size have shown that the vibrational energy flows from a solute to solvent molecules on a picosecond time scale and is completely lost after an  $\approx 20$  ps delay time in most solutions. This suggests that the vibrational relaxation dynamics in the cell is quite different from that of the solute–solution system. We assumed that the vibrational relaxation of Rhodamine 6G in the cell is greatly influenced by the neighboring environment. Inside the cell is a nonuniform environment, because it consists of many parts, such as a nucleus, a cytoplasm, and a cell membrane, which interact with each other or water molecules in the cell. This may cause the site dependence of vibrational relaxation in a cell. In order to understand the more detailed characteristic dynamics in a cell, vibrational relaxation of specific parts in a cell, such as the nucleus, cytoplasm, and cell membrane, will be measured by using other probe fluorescent dyes, such as SYTO24, Dio18, and Alexa 488 in the next step.

In conclusion, we succeeded to perform TFD-IR imaging of *A. thaliana* roots by using a nonscanning two-color IR super-resolution microscope. We also demonstrated picosecond time-resolved TFD-IR imaging of the vibration relaxation of Rhodamine 6G in *A. thaliana* roots and found an abnormally long-lived component on vibrational relaxation in a cell. This may cause a site dependence of the vibrational relaxation in a cell. These results show a possibility that the nonscanning two-color IR super-resolution microscope will be useful for mapping a specific IR absorption with high spatial resolution and the observation of dynamics in a nonuniform environment, such as a cell.

The present work was in part financially supported by a Grant-in-Aid for Scientific Research (KAKENHI) on Priority Areas [432] MEXT, Japan.

## References

- G. J. Puppels, F. F. M. De Mul, C. Otto, J. Greve, M. Robert-Nicoud, D. J. Arndt-Jovin, T. M. Jovin, *Nature* **1990**, *347*, 301.
- Y.-S. Huang, T. Karashima, M. Yamamoto, T. Ogura, H. Hamaguchi, *J. Raman Spectrosc.* **2004**, *35*, 525.
- H. Kano, H. Hamaguchi, *Chem. Lett.* **2006**, *35*, 1124.
- M. Born, W. Wolf, in *Principle of Optics*, 7th ed., Cambridge Univ. press, Cambridge, **1997**.
- A. Seilmeier, W. Kaiser, A. Laubereau, S. F. Fischer, *Chem. Phys. Lett.* **1978**, *58*, 225.
- M. Sakai, M. Fujii, *Chem. Phys. Lett.* **2004**, *396*, 298.
- M. Sakai, Y. Kawashima, A. Takeda, T. Ohmori, M. Fujii, *Chem. Phys. Lett.* **2007**, *439*, 171; M. Sakai, T. Ohmori, M. Fujii, in *Nano Biophotonics*, ed. by H. Masuhara, S. Kawata, F. Tokunaga, Elsevier, Oxford, **2007**, pp. 189–195.
- T. Elsaesser, W. Kaiser, *Annu. Rev. Phys. Chem.* **1991**, *42*, 83.
- H. Hamaguchi, T. L. Gustafson, *Annu. Rev. Phys. Chem.* **1994**, *45*, 593; K. Iwata, H. Hamaguchi, *J. Raman Spectrosc.* **1994**, *25*, 615.
- R. J. Sension, A. Z. Szarka, R. M. Hochstrasser, *J. Chem. Phys.* **1992**, *97*, 5239; Y. Mizutani, T. Kitagawa, *Science* **1997**, *278*, 443; H. Okamoto, T. Nakabayashi, M. Tasumi, *J. Phys. Chem. A* **1997**, *101*, 3488; M. Sakai, M. Mizuno, H. Takahashi, *J. Raman Spectrosc.* **1998**, *29*, 919; D. D. Dlott, *Chem. Phys.* **2001**, *266*, 149.